Control of Non-Inductive Current in Heliotron J

K. Nagasaki[1)], G. Motojima[2)], M. Nosaku[2)], H. Okada[1)], T. Mizuuchi[1)], S. Kobayashi[1)], K. Sakamoto[1)], K. Kondo[2)], Y. Nakamura[2)], H. Arimoto[2)], S. Watanabe[2)], S. Matsuoka[2)], T. Tomokiyo[2)], K. Y. Watanabe[3)], A. Cappa[4)], F. Sano[1)]

1) Institute of Advanced Energy, Kyoto University, Uji, Kyoto 611-0011, Japan
2) Graduate School of Energy Science, Kyoto University, Uji, Kyoto 611-0011, Japan
3) National Institute for Fusion Science, Toki, Gifu 509-5292, Japan
4) Laboratorio Nacional de Fusión, EURATOM-CIEMAT, Madrid, Spain

e-mail contact of main author: nagasaki@iae.kyoto-u.ac.jp

Abstract. Non-inductive current of electron cyclotron heated (ECH) plasmas has been examined in the helical axis heliotron device, Heliotron J. The bootstrap and EC currents are separated by comparing the experiments with positive and negative magnetic field. The estimated bootstrap current is found to be affected by the magnetic field configuration. It increases with an increase in the bumpy component of the magnetic field spectrum, which agrees well with a neoclassical prediction using the SPBSC code. The EC current driven by oblique launch with respect to the magnetic field strongly depends on the field configuration and the EC power deposition location. The EC current is enhanced when the EC power is deposited on the magnetic axis. The maximum EC current and current drive efficiency are I_{EC} = -4.6 kA, $\eta = n_e R I_p / P_{EC} = 8.4\times10^{16}$ A/Wm^2, respectively. The EC current changes its flowing direction depending on the magnetic field ripple structure where the EC power is deposited.

1. Introduction

Control of non-inductive toroidal current is one of key issues to realize high performance plasmas in toroidal fusion devices. In helical systems, the toroidal current such as Ohmic current is not required for plasma equilibrium since the confinement magnetic field is generated by external coils. However, finite plasma pressure inherently drives non-inductive current, so called bootstrap current, which affects the equilibrium and stability due to the change in rotational transform. The bootstrap current has been experimentally studied in CHS [1], LHD [2] and W7-AS [3] with regards to transport and MHD stability. Theories predict that the bootstrap current can be suppressed by optimizing the magnetic field spectrum [4][5]. From the diagnostic point of view, helical systems are advantageous to precise measurement of the total plasma current because of no inductive current. Small current of less than 1 kA is possible to measure by using conventional Rogowski coils.

Electron cyclotron current drive (ECCD) is recognized as a useful scheme for controlling rotational transform and magnetic shear related to the heat/particle transport, equilibrium and stability. In helical systems, ECCD is considered to suppress the bootstrap current in order to tailor the current density profile. Furthermore, the detailed study on ECCD in helical system deepens our understanding of the ECCD physics in toroidal devices. ECCD in helical systems was measured first in W7-AS [6]. Although the sophisticated investigation was performed, the EC current was estimated by applying some theoretical results, that is, the EC current was obtained by substituting the calculated inductive and bootstrap currents from total current experimentally measured. Net plasma current was maintained to be zero in order to avoid the effect of low-order rational values at the plasma edge degrading the confinement properties.

In Heliotron J, we have experimentally estimated the EC current without using any numerical calculation. No significant degradation of plasma confinement has been observed in the ECH plasmas reported in this paper.

The objective of this paper is to study experimentally the properties of the non-inductive toroidal current in ECH plasmas. A helical-axis heliotron device, Heliotron J, has high flexibility to control the magnetic field configuration, making it possible to investigate the properties of the bootstrap and EC currents in a wide range of magnetic field configurations. The organization of this paper is as follows. The experimental setup is described in Sec. 2. The experimental results on non-inductive current are shown in Sec. 3. The dependence of the bootstrap and EC currents on the magnetic configuration and the EC power deposition is discussed. Conclusions are given in Sec. 4.

2. Experimental setup

Heliotron J is a medium sized plasma experimental device [7]. The device parameters are as follows; the plasma major radius, R = 1.2 m, the averaged minor radius, a = 0.1-0.2 m, the rotational transform, $\iota/2\pi$ = 0.3-0.8, and the maximum magnetic field strength on the magnetic axis, B_0 = 1.5 T. The coil system is composed of an L=1, M=4 helical coil, two types of toroidal coils A and B, and three pairs of vertical coils. The Heliotron J device provides a wide variety of magnetic configuration by changing the current ratios in each coil. In particular, the bumpiness component, which is introduced as a third knob to control neoclassical transport, is changed by controlling the currents in toroidal coils A and B. Three configurations are chosen, that is, $\varepsilon_b=B_{04}/B_{00}$ at ρ = 0.67 as 0.01 (low bumpiness), 0.06 (medium bumpiness) and 0.15 (high bumpiness) with keeping the toroidicity, helicity, rotational transform and plasma volume almost fixed. Here B_{mn} is the Fourier component of the magnetic field strength in the Boozer coordinates.

The total toroidal current is measured by Rogowski coils wound on the inner wall of the poloidal cross-sections at two different toroidal angles, that is, the corner and the straight sections. We confirmed that the toroidal current by two Rogowski coils was almost the same. The resistive current diffusion time is about 100 msec in the Heliotron J plasma parameters. In the experiment reported here, the measured toroidal current is saturated within the pulse length at $n_e > 0.5\times10^{19}$ m^{-3}, but it continues to rise up during the discharge at lower density so that the current is underestimated in low density regime.

A 70 GHz ECH system [8] is used for studying the non-inductive current in Heliotron J. Plasmas are produced and heated by the 70GHz second harmonic X-mode ECH for which the cut-off density is 3.0×10^{19} m^{-3}. The injected power is up to 350 kW, and the maximum pulse length is 120 msec in the experiment reported here. The unfocused Gaussian beam is launched from the top of the torus at the straight section where the flux surfaces are bean-shaped, and the B-contour forms a saddle-type profile. Although the wave beam is injected perpendicularly with respect to the equatorial plane, it crosses the resonance layer obliquely because of the 3-D magnetic field structure, resulting that the finite parallel refractive index, $N_{\parallel}$ = 0.44, drives the EC current. The polarization can be controlled from the X-mode to the O-mode by a linear polarizer installed in a miter bend. In the ECH experiment,

the central electron and ion temperatures range 0.3-1.0 keV and 0.15-0.2 keV, respectively.

A poloidal cross-section in medium bumpiness configuration is shown in Fig. 1, from which the EC beam is launched. The magnetic field, B = 1.25 T, is located at the magnetic axis at ω_0/ω =0.50. Here, ω_0 and ω are the electron cyclotron frequency on the axis in the straight section and the injected wave frequency, respectively. A ray tracing calculation using the TRECE code [9] shows that the EC power is deposited at off-axis of ρ = 0.2 due to the Doppler shift resonance, $\omega - k_{\|}v_{\|} = 2\omega_{ce}$. When the magnetic field strength is set lower as ω_0/ω = 0.49, the resonance layer moves toward the helical coil so that the EC power can be deposited at on-axis. Electron cyclotron emission diagnostic using a multi-channel radiometer confirms that centrally peaked T_e profile was formed at ω_0/ω = 0.49. Transmitted wave measurements [10] shows that the single pass absorption rate is estimated about 90 % consistent with the ray tracing results, indicating the single pass absorption has main contribution to plasma heating.

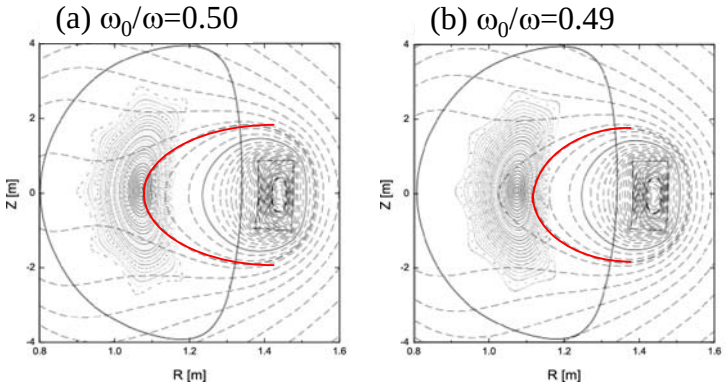

FIG. 1. Poloidal cross-sections of ECH injection port at (a) ω_0/ω = 0.50 and (b) ω_0/ω = 0.49. The solid line corresponds to the magnetic field strength, B = 1.25 T.

3. Experimental results

3.1 Separation of bootstrap current and EC current

Figure 2 shows the dependence of the measured toroidal current on the line averaged electron density at ω_0/ω = +0.50 and ω_0/ω = -0.50 at medium bumpiness configuration. Here the sign denotes the clockwise and counter-clockwise direction of magnetic field looking from the top of the torus. The positive current flows in the paramagnetic direction for positive magnetic field, increasing the rotational transform. It is noted that the achievable density is typically $n_e \sim 2.0\times10^{19}$ m^{-3}, limited by radiation collapse. In ECH plasmas, the toroidal current is composed of the bootstrap current and the EC current. They can be separated by comparing the experimental results between positive and negative magnetic fields, since the flow direction of the bootstrap current is changed by reversing the magnetic field, while that of the EC current is not. The bootstrap current, I_{BS}, and the EC current, I_{EC}, are estimated by the following equations,

$$I_{BS} = \frac{I_p^{cw} - I_p^{ccw}}{2},$$

$$I_{EC} = \frac{I_p^{cw} + I_p^{ccw}}{2},$$

where I_p^{cw} and I_p^{ccw} are the toroidal current at positive (clockwise) and negative (counter-clockwise) magnetic field experiments, respectively. Here we assume that nonlinear interaction between the bootstrap and EC currents is negligible. We confirmed that the other

plasma parameters such as stored energy were almost the same for both experiments. The bootstrap current increases with the electron density due to the increase in plasma pressure gradient, but it is saturated at $n_e > 1.0\times10^{19}$ m^{-3}. The plasma becomes more collisional with electron density, giving rise to the suppression of the bootstrap current. The EC current is less driven for the whole density region under this condition. According to the VMEC equilibrium calculation, the rotational transform is modified by the non-inductive current. For example, the central rotation transform is drastically decreased from 0.56 to 0.19 when a current of -5 kA is localized at the magnetic axis likely as ECCD. The rational numbers such as 4/7 and 4/8 appear, forming natural islands in the confinement region. Nevertheless, no significant degradation of plasma confinement due to the change in rotational transform has been observed experimentally, although modification of the edge structure has been observed [11].

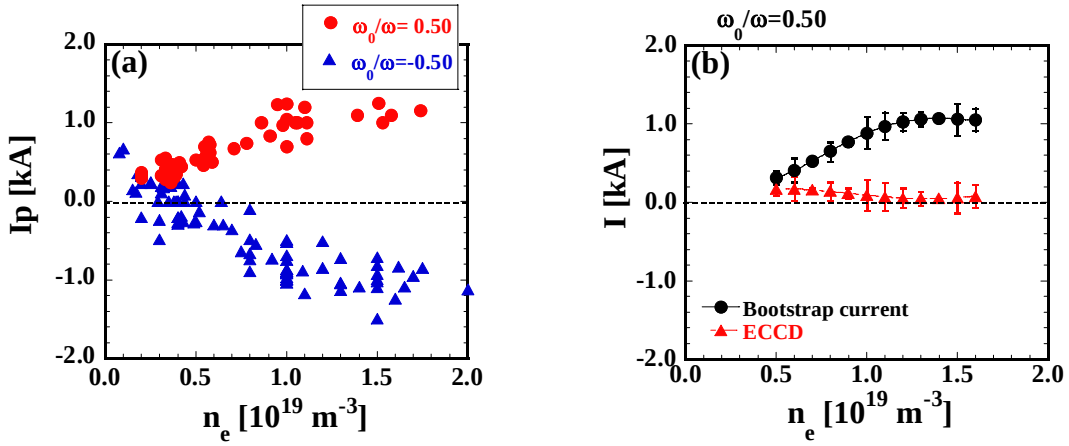

FIG. 2. Density dependence of non-inductive current at medium configuration, (a) measured total toroidal current at ω_0/ω = +0.50 and ω_0/ω = -0.50, (b) estimated bootstrap and EC currents.

3.2 Bootstrap current

The behavior of the bootstrap current has been studied by changing the bumpiness component in order to investigate the effect of the field configuration [12]. The resonance location is fixed at $\omega_0/\omega = 0.50$ in which the bootstrap current is dominant and the contribution of ECCD is weak. Figure 3 shows the observed toroidal current as a function of the electron density for three bumpiness cases. The bootstrap current is dependent on the pressure and temperature gradient. For all the configurations, the toroidal current increases with electron density and becomes gradually saturated. The bootstrap current tends to flow more at high bumpiness configuration. The experiment of scanning the EC power deposition position with the configuration fixed shows that the bootstrap current is insensitive to the EC power deposition location. This is related to the fact that the bootstrap current flow at off-axis where the pressure gradient is large. The change in T_e profile at the core region does not affect the total bootstrap current so much.

The toroidal current at $n_e = 1.0\times10^{19}$ m^{-3} against the bumpiness is shown in Fig. 4. Plotted are also theoretical predictions calculated by the SPBSC code [5]. In the SPBSC code, a connection formula from 1/ν to Pfirsch-Schluter collisional regime is applied, and the bootstrap current is calculated based on a momentum method for axisymmetric devices. The density and temperature profiles are chosen to be consistent with the plasma stored energy

experimentally measured. We assume the electron density as $n_e = n_e(0)(1-\rho^6)$, $n_e(0) = 1.0\times10^{19}$ m^{-3}, and the electron and the ion temperature as $T_e = T_e(0)(1-\rho^2)^2$, $T_e(0)$ = 600-700 eV, $T_i = T_i(0)(1-\rho^2)^2$, $T_i(0)$ = 150-200 eV, respectively. No radial electric field is applied in this calculation although it may affect the bootstrap current particularly in low collisional regime. The magnitude and flow direction of the observed toroidal current is in good agreement with the neoclassical prediction. The agreement with the neoclassical calculation is also found at low density, $n_e = 0.5\times10^{19}$ m^{-3}, except for low bumpiness configuration. Although the reason for the discrepancy is not clear yet, it may be because the radial electric field is enhanced in the collisionless regime, and/or because the EC current flows in the counter-clockwise direction.

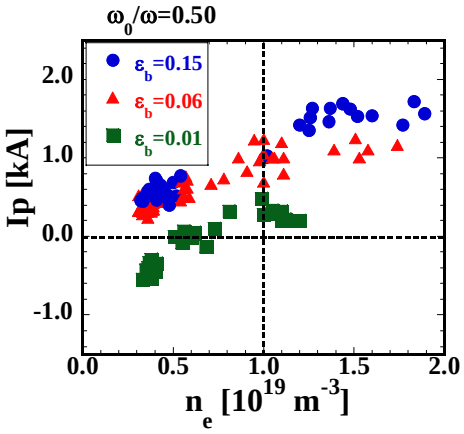

FIG. 3. Density dependence of measured toroidal current at three bumpiness configurations.

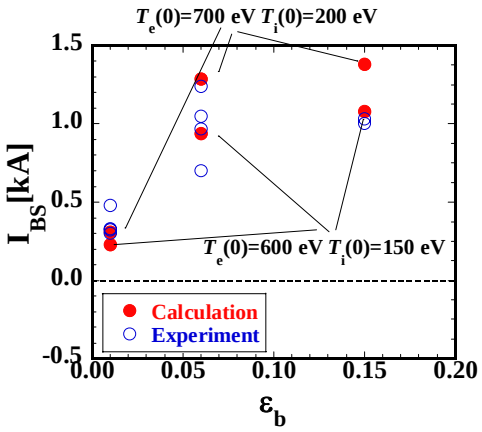

FIG. 4. Bootstrap current as a function of bumpiness. The electron density is n_e = 1.0×10^{19} m^{-3}, and the magnetic field strength is ω_0/ω = 0.50 so that the bootstrap current can be dominant.

The bumpiness reduces the bootstrap current in helical plasmas since it breaks the symmetry in the magnetic field configuration. However, the mechanism driving the bootstrap current is complicated if some other components are included in the magnetic field as well as the bumpiness. The dominant term in the geometric factor, G_{bs}, at asymmetric configuration is a function of the poloidal angle θ_{max} where the magnetic field strength has its maximum value. θ_{max} can be changed by the bumpiness and affects toroidal and helical trapped particles, resulting in the change of G_{bs}. This means that bumpiness which makes θ_{max} change plays an important role on the direction of the bootstrap current.

3.3 ECCD

The amount of EC current depends on the EC power deposition. The density dependence of the bootstrap and EC currents is shown in Fig. 5. The configuration is the same as Fig. 2, but the resonance position is different, ω_0/ω = +0.49. It can be seen that the bootstrap current has the same tendency, but the EC current flows more. Figure 6 shows the observed toroidal current as a function of ω_0/ω. The electron density is set as low as $n_e = 0.5\times10^{19}$ m^{-3} so that the EC current can be dominant. Around ω_0/ω = 0.49, a large toroidal current has been observed, and the flow direction is changed by the bumpiness conditions. In low bumpiness configuration, the plasma can not be produced at $\omega_0/\omega < 0.486$ since the single pass X-mode

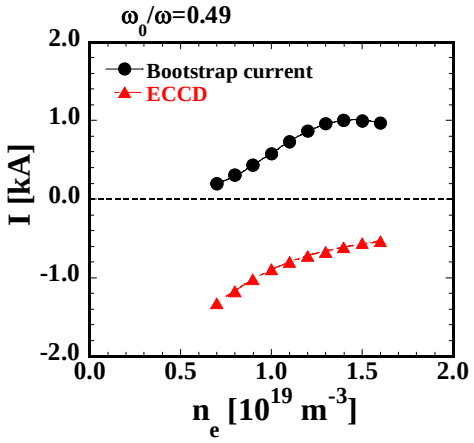

FIG. 5. Dependence of bootstrap current and ECCD on line averaged electron density at ω_0/ω = 0.49 in ECH plasmas.

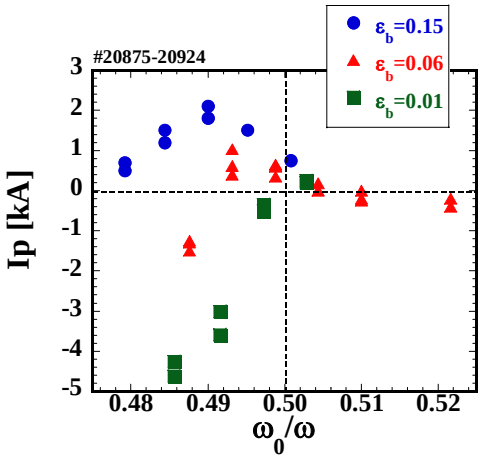

FIG. 6. Magnetic field strength dependence of toroidal current with bumpiness.

fraction is decreased due to the saddle type magnetic field structure.

In order to clarify the reason for the change in toroidal current direction, the bootstrap current and the ECCD are separated at ω_0/ω = 0.49. Figure 7 shows the density dependence of the EC current. The positive EC current is driven at high bumpiness, while the positive EC current is driven at low bumpiness. The decrease in EC current at $n_e < 0.2\times10^{19}$ m^{-3} is due to the reduction of single pass absorption. The maximum toroidal current of -4.6 kA has been observed at low bumpiness configuration, which is higher than the current including the bootstrap current and NB currents in NBI plasmas at high density of $n_e > 2.0\times10^{19}$ m^{-3}. The maximum current drive figure of merit is $n_eRI_p/P_{EC} = 8.4\times10^{16}$ A/Wm^2 (I_p = 3.2 kA, $n_e = 0.7\times10^{19}$ m^{-3} and P_{EC} = 320 kW). Here we take the injection power as EC power. This current drive efficiency is lower than linear theory, suggesting that the linear approach is not valid for 3-D magnetic field structure of Heliotron J.

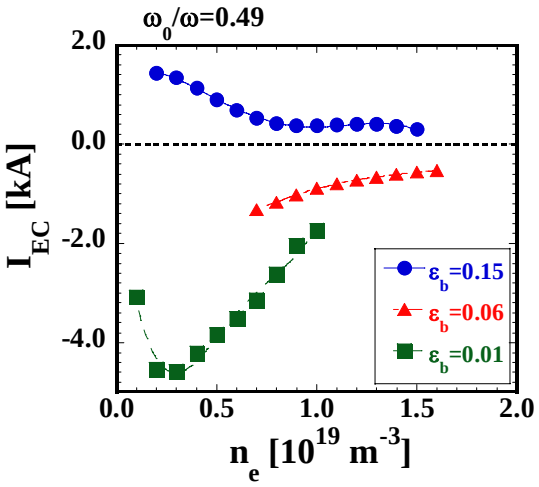

FIG. 7. Dependence of ECCD on line averaged electron density at ω_0/ω = 0.49 in ECH plasmas.

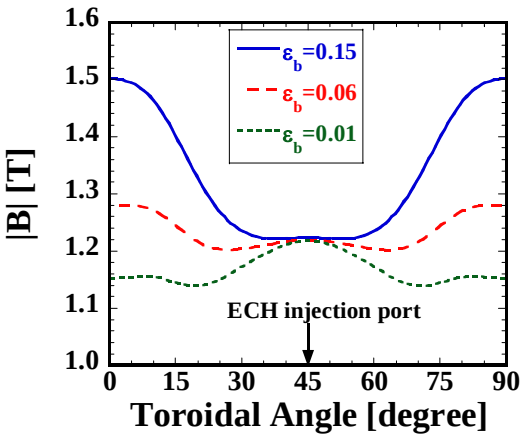

FIG. 8. Magnetic field strength along magnetic axis. The arrow denotes the EC wave injection position.

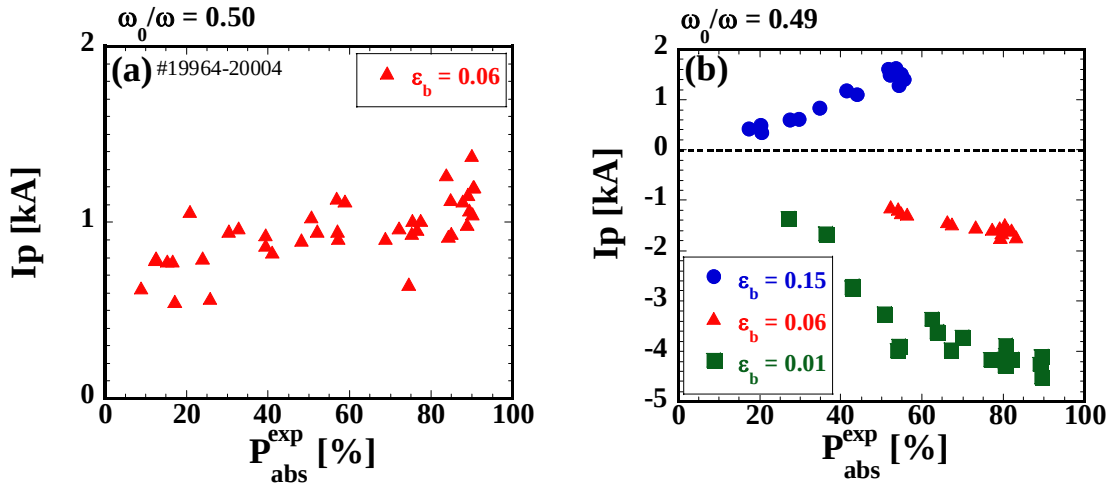

FIG. 9. Dependence of measured toroidal current on single pass absorption, (a) bootstrap current dominant case, ω_0/ω = 0.50 and n_e = 1.0×10^{19} m^{-3} and (b) EC current dominant case, ω_0/ω = 0.49 and n_e = 0.5×10^{19} m^{-3}.

One reason for the current reversal is that velocity space effects are responsible for the ECCD. The Fisch-Boozer effect [13] considers the perpendicular excursion in velocity of a group of electrons with positive $v_{||}$. Acceleration of these electrons causes an excess of electrons with positive $v_{||}$, resulting in a current in the negative toroidal direction. On the other hand, the Ohkawa effect [14] drives current in the direction opposite to the Fisch-Boozer current. Asymmetry in $v_{||}$ is lost due to bouncing in the magnetic ripple, and a deficit in velocity space generates an electrical current in the positive toroidal direction. As shown in Fig. 8, the electrons are heated at the ripple top in low bumpiness configuration, and hence the Fisch-Boozer effect is strong. On the other hand, in high bumpiness configuration, the electrons are accelerated at the ripple bottom, and they tend to be trapped particles, making the Ohkawa effect stronger. These qualitative predictions are consistent with the measured ECCD direction. The Ohkawa effect is comparable to the Fisch-Boozer effect in Heliotron J, and the ECCD direction is determined by the balance between them.

The X-mode fraction has been changed by polarization control angle in order to determine the role of single pass absorption as shown in Fig.9. The single pass absorption rate is estimated by using transmitted EC waves. The bootstrap current, which is dominant at ω_0/ω = 0.50, is insensitive to the single pass absorption. On the other hand, the EC current decreases with the decrease in X-mode fraction for all three configurations, indicating that the ECCD is driven by the single pass absorption. This is a reasonable result since multi-reflected waves randomize the parallel refractive index, and hence they do not contribute to the ECCD.

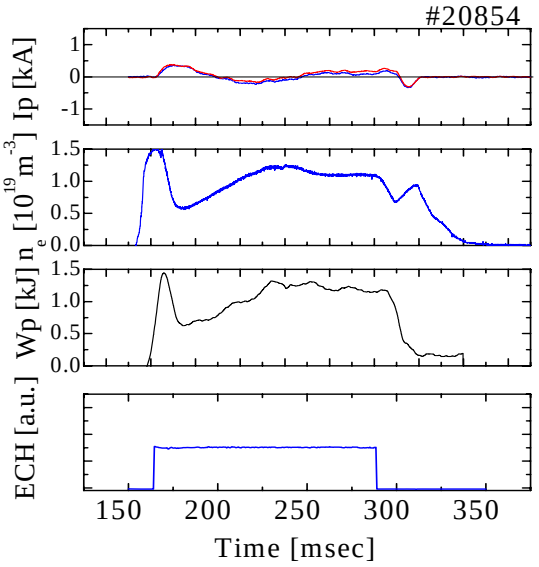

FIG. 10. Time evolution of ECH plasma with net free current.

The bootstrap current can be cancelled by ECCD. Figure 10 shows a time evolution of the toroidal current, the electron density and the plasma stored energy at ω_0/ω =0.49 and low bumpiness. Net zero current state ($|I_p| < 0.4$ kA) is maintained during the discharge by controlling the ECCD location. Although local cancellation may not be fully realized by ECCD because of their different current profile shapes, the EC current is comparable with the bootstrap current, and the ECCD has a potential to tailor the rotational transform profile to avoid rational numbers in rotational transform.

4. Conclusions

Non-inductive current including the bootstrap and EC driven currents has been studied in Heliotron J ECH plasmas. The non-inductive current of less than 1 kA is accurately measured. The bootstrap current and the EC current are clearly separated by the magnetic field reversal experiment. The experimental results show that the bootstrap current increases with plasma pressure, and it depends on the magnetic field configuration, particularly on the bumpiness. It agrees well with the neoclassical prediction using the SPBSC code which takes account of the configuration effect. The ECCD is enhanced when the EC power is deposited on the magnetic axis. The EC current flows in the toroidal direction predicted by linear theory at low bumpiness configuration where the EC power is deposited at the ripple top of the magnetic field. On the other hand, the flow direction is reversed at low bumpiness configuration where the EC power is deposited at the ripple bottom. These experiments indicate that ECCD is determined by the competition between the Fisch-Boozer and Ohkawa effects. Net current-free state has been demonstrated by compensating the bootstrap current with the EC current. Quantitative theoretical analysis considering the trapped electron effect in real 3-D field structure is left for future.

Acknowledgement
The authors are grateful to the Heliotron J staff for operating the device.

References

[1] ISOBE, M., et al., Plasma Phys. Control. Fusion **44** (2002) A189-A195.
[2] FUJIWARA, M., Nucl. Fusion 39 (1999) 1659-1666.
[3] SALLANDER, E., et al., Nucl. Fusion **40** (2000) 1499-1509.
[4] NAKAMURA, Y., et al., Fusion Sci. Technol. **50** (2006) 281-286.
[5] WATANABE, K. Y., et al, Nuclear Fusion **35** (1995) 335-345.
[6] ERCKMANN, V., et al., Fusion Eng. Design **53** (2001) 365-375.
[7] OBIKI, T., et al., Nucl. Fusion **41** (2001) 833-844.
[8] SHIDARA, H., et al., Fusion Sci. Technol. **45** (2004) 41-48.
[9] TRIBALDOS, V., et al., J. Plasma Fusion Res. **78** (2002) 996.
[10] NAGASAKI, K., et al., Proc. 14th Joint Workshop on ECE and ECRH, May 2006, Santorini island, Greece.
[11] MIZUUCHI, T., et al., this conference EX/P4-18
[12] MOTOJIMA, G., et al., Accepted for Fusion Sci. Technol.
[13] FISCH, N. J. and BOOZER, A. H., Phys. Rev. Lett. **45** (1980) 720-722.
[14] OHKAWA, T., General Atomics Report GA-A13847 (1976)